IceCube in SNOwGLoBES (working draft - v1)

B.J. Felix Malmenbeck - felixm@kth.se

October 19, 2018

1 Introduction

1.1 General overview

One important aspect of defining an experiment in SNOwGLoBES is determining the experiment's detector mass, which acts as an overall scale factor. In the case of IceCube, the array's great size and lack of well-defined borders makes the mass of the detector somewhat ambiguous. IceCube has digital optical modules (DOMs) spread out over a volume of about $1\,\mathrm{km}^3$, with no optically opaque boundary layer between them. However, the likelihood that a given event will be observed drops off with its distance to the nearest DOM.

The distance from which an interaction event can be observed is also dependent on the energy of the incoming neutrino. As such, a high-energy cosmic ray neutrino may produce a signal across multiple detectors, allowing for the identification and reconstruction of single events, whereas the light produced by supernova neutrinos often fades below the detection threshold without triggering a single detector.

Fig. 1 shows the result of an event-by-event simulation of 10 million neutrino interactions. While interaction events occuring at a given depth are expected to be uniformly distributed in the horizontal xy-plane, detected events are clustered near the detectors, which show up as vertices in a hexagonal lattice.

As such, a detailed simulation of IceCube must take the spatial distribution of detected devents into account. However, such simulations are very resource-intensitve. With the SNOwGLoBES implementation of IceCube, our focus is to enable computationally light calculations of expected event rates.

To accomplish this, we associate with each detector an energy-dependent effective volume, allowing us to model IceCube by analogy with a smaller detector with perfect event detection. This process will be detailed in Section 2.

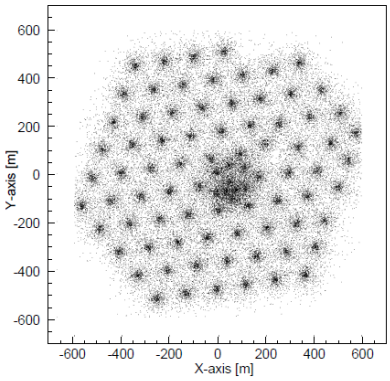

Figure 1: The spatial distribution of detected supernova neutrino events, simulated using GEANT-3.21. Each dot represents a interaction event which was registered by a digital optical module. (Abbasi et al., 2011)

1.2 Applying custom parameters

When simulating a given experiment, some users may wish to adjust certain performance-related parameters (such as the number of active detectors) on their own, or apply their own post-processing method to adjust for features such as data screening technique (such as HitSpool). However, others will be satisfied with a rough estimate, and may not wish to expend time perusing this documentation or writing additional code. As such, in the interest of avoiding the spread of overly optimistic data, we have included conservative estimates in the form of multiplicative factors modifying the total event rates. These have been approximated as constants, rather than as functions of energy, so that users wishing to achieve a more detailed analysis can easily divide the rates by these factors before applying their own calculations.

These factors are:

- **Number of active detectors:** $N_{DOM} \doteq 0.98 \times 5160$ (detailed in §2.1.1)
- **Dead time efficiency:** $\epsilon_{deadtime} \doteq 0.95$ (detailed in §2.1.2)

2 Calculating effective volume

2.1 Total effective volume

The effective volume for any given DOM depends on the species of interaction product $e^{\pm}$and on the energy E' at which they are produced.

The total effective volume for the full detector array and a given interaction product $e^{\pm}$ is provided by the formula

$$V_{eff,\pm}(E') = N_{DOM}\epsilon_{deadtime}v_{\bar{eff},\pm}(E') \qquad (1)$$

where $v_{eff,\pm}^{-}(E')$ is the average effective volume of a single DOM, while the factors N_{DOM} and $\epsilon_{deadtime}$ together represent how many detectors are producing useful data at any given time.

2.1.1 Number of active detectors - N_{DOM}

The quantity $N_{DOM} = \rho_{active} \times 5160$ is the number of active digital optical modules which are taking measurements at the time of the experiment. For this implementation, we have defined $\rho_{active} \doteq 0.98$, reflecting an assumption that 2% of all detectors are either inactive at the time of the signal or are excluded from the final analysis because they appear to be providing erroneous data. This assumption mirrors the one applied in (Abbasi et al., 2011).

2.1.2 Dead time efficiency - $\epsilon_{deadtime}$

Noise is significant issue when dealing with low-energy neutrinos. On top of random background noise, there are also pulses of increased noise immediately following each detector event. There are different ways of mitigating the effect of this correlated noise, one of which is the introduction of an artificial dead time τ after each detector event, during which further hits are excluded from the analysis. This results in reduced noise at the cost of a reduced signal. In (Abbasi et al., 2011), this effect is approximated by the dead time efficiency factor

$$\epsilon_{deadtime}(t) \approx \frac{0.87}{1 + \tau \cdot r_{SN}(t)}, \tag{2}$$

where $r_{SN}(t)$ is the signal rate at time t and $\tau = 250\,[\mu s]$.

Because the smearing and post-smearing files in SNOwGLoBES are only dependent on energy, and not on time or signal rate, this calculation cannot be natively supported within the package. Furthermore, doing so would make it difficult for those wishing to use other methods for dealing with noise, or for those wishing to use different values for the artificial deadtime.

As such, the experiment files apply a constant value $\epsilon_{deadtime} \doteq 0.95$ to the effective volume calculation. This value was selected to approximate the total effect on the signal once HitSpool data has been analyzed. However, if one is interested in the data which will be more immediately available to experimenters via SNDAQ, a better approximation will be given by Eq. 2. As is illustrated in Fig. 2, the value of $\epsilon_{deadtime}(t)$ varies both with time and with flux model. This affects both the total event rate and its time evolution.

To illustrate the effect on total effect rate, we have calculated the ratio $\rho_{deadtime}$ between the total event rate, $r_{tot} = \int_{-20\,[ms]}^{497.5\,[ms]} r(t)dt$, and the event rate with the effect of deadtime neglected, $r_{*,tot} = \int_{-20\,[ms]}^{497.5\,[ms]} r_*(t)dt$. The result

is illustrated in Fig. 3, using data obtained from (O'Connor & Ott, 2013-**Dataset**). We find that a value of $\epsilon_{deadtime} = 0.8$ underestimates the total event rate for 95% of the considered cases, including for all cases with compactness $\xi_{1.75} \leq 1.256$.

2.2 Effective volume per DOM

When calculating the effective volume per DOM, we have followed the process described in (Kowarik, 2010). With respect to detection of interaction products $e^{\pm}$, each detector contributes an average effective volume

$$\bar{v}_{eff,\pm}(E') = d_{\pm}(E')\frac{dN_\gamma}{dx}\bar{v}_{eff,\gamma} \tag{3}$$

where:

$d_{\pm}(E') = C_{\pm}\theta(E' - E_{ch}) \cdot (E' - E_{ch})$ is the path traveled by an interaction product $e^{\pm}$ before its (total) energy falls below the Cherenkov energy threshold $E_{ch} = m_e + 0.272\,[MeV] = 0.783\,[MeV]$. θ is the Heaviside step function. The factor $C_{\pm}$ quantifies a small difference in the behavior of positrons and electrons, with values $C_+ = 0.577\left[\frac{cm}{MeV}\right]$ and $C_- = 0.580\left[\frac{cm}{MeV}\right]$.

$\frac{dN_\gamma}{dx}$ is the rate at which photons with wavelengths between $300\,[nm]$ and $600\,[nm]$ are radiated by the charged lepton as it moves through the ice. As per (Kowarik, 2010), this rate can be calculated by use of the Frank-Tamm formula:

$$\frac{dN_\gamma}{dx} = \int_{300\,[nm]}^{600\,[nm]} d\lambda \frac{d^2N_\gamma}{dxd\lambda} = \int_{300\,[nm]}^{600\,[nm]} d\lambda \frac{2\pi\alpha}{\lambda^2}\left(1 - \frac{1}{\beta^2 n(\lambda)^2}\right) \tag{4}$$

With the approximations $n(\lambda) \approx n_{ice}(400\,[nm]) = 1.3195$ and $\beta \approx 1$, and $\alpha \approx \frac{1}{137}$ being the fine structure constant, we find that

$$\frac{dN_\gamma}{dx} \approx 2\pi\alpha\left(1 - \frac{1}{1.3195^2}\right)\left[\frac{1}{300\,[nm]} - \frac{1}{600\,[nm]}\right] \approx 325,35\,[cm^{-1}].$$

Lastly, $\bar{v_{eff,\gamma}} = 0.1575\,[m^3]$ is the mean effective volume for photons in the IceCube ice, which has been calculated through simulations (Kowarik, 2010).

3 Cross sections

SNOwGLoBES expresses the differential cross section as a product of the total cross section and an energy resolution function:

$$\frac{\sigma_I(E, E')}{dE'} = \sigma_I(E)k_f(E', E) \tag{5}$$

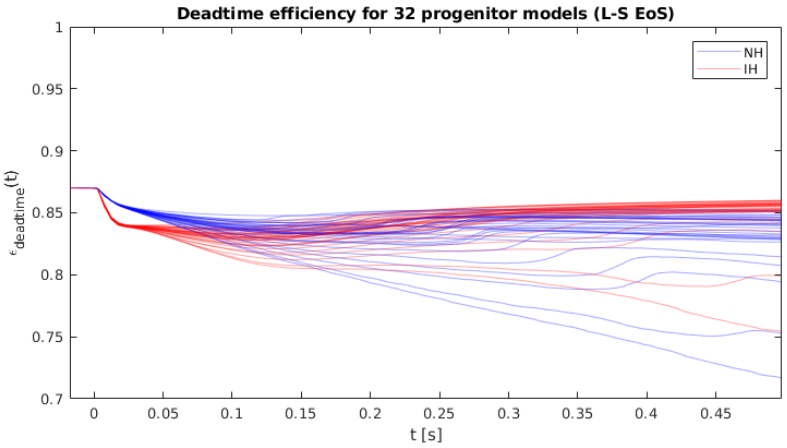

Figure 2: *Deadtime efficiency factor as a function of time for 32 different progenitor models using the 1-dimensional Lattimer-Swesty equation of state, with progenitor masses between 12 and 120 solar masses.* $\epsilon_{deadtime}(t)$ *was calculated using event rates obtained from SNOwGLoBES for two different mass hierarchies and at* $d = 10\,[kpc]$*. SNOwGLoBES fluency data was obtained from (O'Connor & Ott, 2013-**Dataset**).*

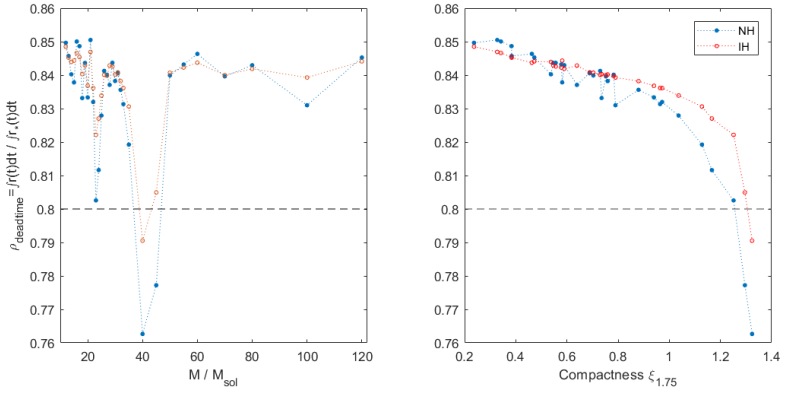

Figure 3: *The effect of the deadtime efficiency factor on the total event rate integrated from* $t = -20\,[ms]$ *to* $t = 497.5\,[ms]$*. SNOwGLoBES fluency data was obtained from (O'Connor & Ott, 2013-**Dataset**). Compactness values were obtained from (O'Connor & Ott, 2013).*

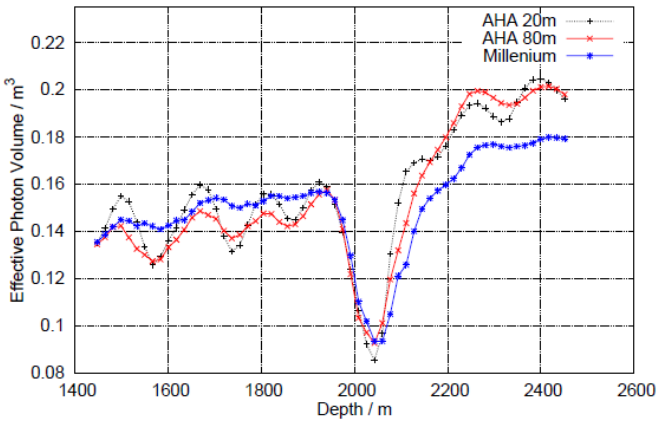

Figure 4: The effective volume of photons as a function of depth, simulated using two different ice models (AHA and Millenium) and at two different resolutions (20m and 80m). The average effective volume was calculated to 0.1575 $[m^3]$ for the AHA 20m model, with an estimated error of $\approx 12\%$. (Kowarik, 2010)

The channels considered in this implementation of IceCube are the same as those which are considered in the Water Cherenkov experiment files which come pre-packaged with SNOwGLoBES v1.2 (Beck, A. et al., 2014). Likewise, we have made use of the pre-packaged total cross section files for all channels. For the interactions involving oxygen atoms, the same smearing files have also been used. For the inverse beta decay and electron scattering channels, new smearing files have been generated using the sources listed in Table 1, selected to agree with (Abbasi et al., 2010).

Interaction	n_{weight}	Partial cross sections
$\bar{\nu}_e + p \rightarrow e^+ + n$	1	Strumia, 2003
$\nu_e + e^- \rightarrow \nu_e + e^-$	5	Marciano, 2003
$\bar{\nu}_e + e^- \rightarrow \bar{\nu}_e + e^-$	5	Marciano, 2003
$\nu_{\mu+\tau} + e^- \rightarrow \nu_{\mu+\tau} + e^-$	5	Marciano, 2003
$\bar{\nu}_{\mu+\tau} + e^- \rightarrow \bar{\nu}_{\mu+\tau} + e^-$	5	Marciano, 2003
$\nu_e + ^{16}\mathrm{O} \rightarrow e^- + \mathrm{X}$	0.5	-
$\bar{\nu}_e + ^{16}\mathrm{O} \rightarrow e^+ + \mathrm{X}$	0.5	-
$\nu_{all} + ^{16}\mathrm{O} \rightarrow \nu_{all} + \mathrm{X}$	0.5	-

Table 1: Channels contributing to the supernova neutrino signal in SNOwGLoBES. Event rates are included for the (time-independent) Livermore and GKVM fluxes included in SNOwGLoBES.

3.1 Neutron capture

In the inverse beta decay interaction channel, the resulting neutron is assumed to undergo neutron capture, $n +^1 H \rightarrow^2 H + \gamma$, resulting in the production of a photon with energy $2.225\,[MeV]$. This photon in turn can undergo Compton scattering, resulting in the production of an electron. Those electrons with an energy above the cherenkov threshold will have an average kinetic energy of $0.951\,[MeV]$. (Kowarik, 2010)

In our experiment files, we have implemented this effect by shifting the positron energy in the energy distribution function by an equivalent amount,

$$E' \mapsto E' + 0.951\,[MeV] \times \frac{C_-}{C_+}\theta(E' - E_{ch}).$$

4 Implementation

4.1 From effective volume to SNOwGLoBES

The event rate for a given interaction channel I with ingoing (anti)neutrino m and interaction product $e^{\pm}$ can be described using the formula

$$r_I(t) = N_{DOM}\epsilon_{deadtime}(t)n_{target}n_{weight,I}\int dE\,\frac{d\Phi_m(t)}{dE}\int dE'\frac{d\sigma_I(E',E)}{dE'}v_{e\bar{f},\pm}(E') \tag{6}$$

When producing "flux" files for use in SNOwGLoBES, one commonly integrates the flux over each time bin $[t_n, t_{n+1}]$ to get the fluence $\frac{d}{dE}F_n(E_\nu) = \int_{t_n}^{t_{n+1}}\frac{d\Phi_m(t)}{dE}\Big|_{E=E_\nu}$.

Furthermore, the integrals $\int dE$ and $\int dE'$ are approximated using sums over energy bins of width $\Delta E = 0.5\,[MeV]$.

Furthermore, rather than the differential cross section, GLoBES makes use of the total cross section $\sigma_I(E_j)$ and in combination with the energy distribution function $k_I(E_k, E_j)$. We thus substitute $\frac{d\sigma_I(E_k,E_j)}{dE'}$ in the above expression with the product $\sigma_I(E_j)k_I(E_k, E_j)$.

Thus, with $E_j = j\Delta E$, we have

$$R_{I,n} = \int_{t_n}^{t_{n+1}} r_I(t) =$$

$$N_{DOM}\epsilon_{deadtime}(t)\rho_{target}n_{weight,I}(\Delta E)^2\sum_{j,k=1}^{200}F_n(E_j)\sigma_I(E_j)k_I(E_k,E_j)v_{e\bar{f},\pm}(E_k) \tag{7}$$

Most of the in Eq. 7 have direct equivalents in SNOwGLoBES experiment files, as is shown in Table 2. What remains is to express the effective volume

of the detector in terms of the experiment's total mass and the post-smearing efficiency $T_f(E_k)$. To do so, we observe that the total number of targets in a mass M is equal to $\rho_{target}\frac{M}{\rho_{ice}}$, whereas the number of targets in volume $V_{eff,\pm}(E_k)$ is equal to $\rho_{target}V_{eff,\pm}(E_k) = \rho_{target}\epsilon_{deadtime}N_{DOM}\bar{v_{eff,\pm}}(E_k)$. We thus define

$$T_f(E_k) = \frac{V_{eff,\pm}(E_k)}{M/\rho_{ice}} = \frac{\epsilon_{deadtime}N_{DOM}\bar{v_{eff,\pm}}(E_k)}{M/\rho_{ice}} \tag{8}$$

File	Quantities	Description
Experiment configuration	M, n_{target}	-
Flux	$F_n(E_j)$	Provided by user
Channels	$n_{weight,I}$	c.f. Table 1
Cross sections	$\sigma_I(E_j)$	c.f. Table 1
Smearing file	$k_I(E_k, E_j)$	$k_I(E_k, E_j) = \frac{1}{\sigma_I}\frac{d\sigma_I(E_k,E_j)}{dE'}$
Post-smearing efficiency	$T_f(E_k)$	$T_f(E_k) = \frac{\rho_{ice}}{M}\bar{v_{eff,\pm}}(E_k)$

Table 2: SNOwGLoBES experiment files and their corresponding quantities in Eq. 7.

The total detector mass M used in Eq. 8 is the same as the value M in the experiment configuration. As such, these two factors will cancel each other out. Therefore, the value of M is largely arbitrary, although it should be selected such that $T_f(E_k) \leq 1$ for all values of $E_k \leq 0.1\,[MeV]$.

4.2 Threshold effects

SNOwGLoBES makes use of 200 equally spaced energy bins with $\Delta E = 0.5\,[MeV]$. As such, the Cherenkov threshold energy $E_{ch} = m_e + 0.272\,[MeV] = 0.783\,[MeV]$ occurs in the middle of the second energy bin, representing the energy interval $0.5\,[MeV] < E' < 1\,[MeV]$. To compensate for this effect, and using the approximation that (anti)electron production is constant in the interval $0.783\,[MeV] < E' < 1\,[MeV]$, we apply a factor $\delta_{thresh} = \frac{1\,[MeV]-E_{ch}}{\Delta E}$ to the post-smearing efficiency for this energy bin:

$$T_f(1\,[MeV]) \mapsto \delta_{thresh}T_f(1\,[MeV])$$

References

[1] Abbasi, R. et al. (IceCube Collaboration), 2011. Astronomy & Astrophysics manuscript no. SN1.22. [arXiv:1108.0171v2]

[2] Kowarik, T., 2010. *Supernova Neutrinos in AMANDA and IceCube: Monte Carlo Development and Data Analysis.* PhD thesis, Mainz U., Inst. Phys.

[3] Beck, A. et al., 2014. *SNOwGLoBES: Supernova Observatories in GLoBES: DRAFT.* `https://github.com/SNOwGLoBES/snowglobes/blob/master/doc/snowglobes_1.2-draft.pdf` [retrieved 2018-07-07]

[4] Strumia, A. & Vissani, F., 2003. Phys. Lett. **B**, 564, 42.

[5] Marciano, W.J. & Parsa, Z., 2003. J. Phys. G: Nucl. Part. Phys., 29, 2629.

[6] P. Huber et al., 2005. Comput. Phys. Commun. 167 (2005) 195. [arXiv:hep-ph/0407333]

[7] P. Huber et al., 2007. Comput. Phys. Commun. 177 (2007). [arXiv:hep-ph/0701187]

[8] O'Connor, E. & Ott, C.D., 2013. ApJ **762** 126 (2013). [arXiv:arXiv:1207.1100v2]
Dataset: *SNOwGLObES fluency data for 5ms bins.* https://sntheory.org/M1prog [retrieved 2018-04-19]